Antiviral efficacy of short-hairpin RNAs and artificial microRNAs targeting foot-and-mouth disease virus

Anabella Currá [1], **Marco Cacciabue** [1], **Maria Jose Gravisaco** [1], **Sebastian Asurmendi** [1], **Oscar Taboga** [Corresp., 1], **Maria I Gismondi** [Corresp. 1]

[1] Instituto de Agrobiotecnología y Biología Molecular (IABiMo), Instituto Nacional de Tecnología Agropecuaria (INTA), Consejo Nacional de Investigaciones Científicas y Técnicas (CONICET), Hurlingham, Buenos Aires, Argentina

Corresponding Authors: Oscar Taboga, Maria I Gismondi
Email address: taboga.oscaralberto@inta.gob.ar, gismondi.maria@inta.gob.ar

RNA interference (RNAi) is a well-conserved mechanism in eukaryotic cells that directs posttranscriptional gene silencing through small RNA molecules. RNAi has been proposed as an alternative approach for rapid and specific control of viruses including foot-and-mouth disease virus (FMDV), the causative agent of a devastating animal disease with high economic impact. The aim of this work was to assess the antiviral activity of different small RNA shuttles targeting the FMDV RNA-dependent RNA polymerase coding sequence (3D). Three target sequences were predicted within 3D considering RNA accessibility as a major criterion. The silencing efficacy of short-hairpin RNAs (shRNAs) and artificial microRNAs (amiRNAs) targeting the selected sequences was confirmed in fluorescent reporter assays. Furthermore, BHK-21 cells transiently expressing shRNAs or amiRNAs proved 70 to >95% inhibition of FMDV growth. Interestingly, dual expression of amiRNAs did not improve FMDV silencing. Lastly, stable cell lines constitutively expressing amiRNAs were established and characterized in terms of antiviral activity against FMDV. As expected, viral replication in these cell lines was delayed. These results show that the target RNA-accessibility-guided approach for RNAi design rendered efficient amiRNAs that constrain FMDV replication. The application of amiRNAs to complement FMDV vaccination in specific epidemiological scenarios shall be explored further.

1 **Antiviral efficacy of short-hairpin RNAs and artificial**

2 **microRNAs targeting foot-and-mouth disease virus**

3 Anabella Currá[1], Marco Cacciabue[1], María José Gravisaco[1], Sebastián Asurmendi[1], Oscar

4 Taboga[1], María Inés Gismondi[1]

5 [1] Instituto de Agrobiotecnología y Biología Molecular (IABIMO), Instituto Nacional de Tecnología

6 Agropecuaria (INTA), Consejo Nacional de Investigaciones Científicas y Técnicas (CONICET),

7 Hurlingham, Buenos Aires, Argentina

9 Corresponding Authors:

10 Oscar Taboga[1]

11 De los Reseros y N. Repetto s/n, Hurlingham, Buenos Aires, 1686, Argentina.

12 Email address: taboga.oscaralberto@inta.gob.ar

14 María Inés Gismondi[1]

15 De los Reseros y N. Repetto s/n, Hurlingham, Buenos Aires, 1686, Argentina.

16 Email address: gismondi.maria@inta.gob.ar

Abstract

RNA interference (RNAi) is a well-conserved mechanism in eukaryotic cells that directs

posttranscriptional gene silencing through small RNA molecules. RNAi has been proposed as an

alternative approach for rapid and specific control of viruses including foot-and-mouth disease

virus (FMDV), the causative agent of a devastating animal disease with high economic impact.

The aim of this work was to assess the antiviral activity of different small RNA shuttles targeting

the FMDV RNA-dependent RNA polymerase coding sequence (3D). Three target sequences

were predicted within 3D considering RNA accessibility as a major criterion. The silencing

efficacy of short-hairpin RNAs (shRNAs) and artificial microRNAs (amiRNAs) targeting the

selected sequences was confirmed in fluorescent reporter assays. Furthermore, BHK-21 cells

transiently expressing shRNAs or amiRNAs proved 70 to >95% inhibition of FMDV growth.

Interestingly, dual expression of amiRNAs did not improve FMDV silencing. Lastly, stable cell

lines constitutively expressing amiRNAs were established and characterized in terms of antiviral

activity against FMDV. As expected, viral replication in these cell lines was delayed. These

results show that the target RNA-accessibility-guided approach for RNAi design rendered

efficient amiRNAs that constrain FMDV replication. The application of amiRNAs to

complement FMDV vaccination in specific epidemiological scenarios shall be explored further.

Keywords

FMDV, antivirals, RNA interference, target accessibility, RNA structure, transgenic cell culture

1. Introduction

Foot-and-mouth disease virus (FMDV) is the causative agent of a highly devastating disease of cloven-hoofed animals leading to enormous economic losses. FMDV belongs to the Aphthovirus genus in the *Picornaviridae* family. There are 7 FMDV serotypes (A, O, C, Asia1, SAT1, SAT2, SAT3) and several subtypes.

The viral particle is ~25-30 nm in diameter and consists of a single stranded (+)RNA molecule surrounded by an icosahedric capsid composed by the four structural viral proteins VP1 to VP4. Viral infection begins with the interaction of the FMDV capsid with cellular receptors (α_V integrins in animal hosts, additionally heparansulfate and a newly identified receptor in cultured cells) (Dicara et al., 2008; Lawrence et al., 2016). Receptor-mediated endocytosis guides the viral particles to the cytoplasm, where the whole replication cycle takes place. Acidification of endosomes drives disassembly of the viral capsid and release of the FMDV genome into the cytoplasm, where it is immediately translated in a cap-independent manner to produce the viral polyprotein. Co- and post-translational processing of the FMDV polyprotein originates viral protein precursors and ultimately the mature structural and non-structural proteins (Grubman & Baxt, 2004). Finally, capsids are assembled and newly synthesized genomes are encapsidated and released from the cell in a lytic way. The replication cycle is fast, taking approximately 6-8 hours in cell culture.

During replication, viral RNA molecules are synthesized by the viral RNA-dependent RNA polymerase (RdRp) 3Dpol. As other viral RdRps, the enzyme lacks proofreading activity, which contributes to the generation of mutated FMDV genomes in every replication cycle. Hence, in an infected host (cell or animal) the virus appears as a swarm of different but closely related viral

64   variants which are called the viral quasispecies (Domingo et al., 2003; Domingo, Sheldon &

65   Perales, 2012; Andino & Domingo, 2015). The quasispecies nature of FMDV facilitates its rapid

66   adaptation to unfavorable environments.

67   Following current standards of the World Organisation for Animal Health (OIE), countries are

68   divided according to their foot-and-mouth disease (FMD) status in FMD-free countries with or

69   without vaccination (almost all Americas, Europe and Oceania) and FMD-endemic countries

70   (parts of Africa and Asia). Current approved FMD vaccines are inactivated viruses formulated

71   with oil-based adjuvants. Although they are effective, inactivated vaccines show a number of

72   disadvantages including lack of cross-protection between serotypes and even subtypes, inability

73   to induce long-lasting immunity (there is a need of re-vaccination to maintain protection) and

74   risk of incomplete inactivation during manufacturing. Moreover, current vaccines take ~7 days to

75   induce protection (Golde et al., 2005). Thus, there is a need of developing new tools against

76   FMDV that may complement vaccination and reduce the risk of infection especially during

77   outbreaks.

78   RNA interference (RNAi) is a well-conserved mechanism in eukaryotic cells that directs

79   posttranscriptional gene silencing (Fischer, 2015). RNAi is mediated through small RNA

80   molecules that guide ribonucleprotein complexes to their cognate mRNAs and lead to their

81   degradation and/or inhibition of translation. There are many types of small RNAs, including

82   microRNAs (miRNAs) and short interfering RNAs (siRNAs). The former are endogenous

83   molecules encoded in the cellular genome that regulate gene expression. In animals, biogenesis

84   of miRNAs involves RNA polymerase II-mediated transcription of a primary miRNA (pri-

85   miRNA), which is further processed by the RNAse III enzyme Drosha to pre-miRNA hairpins.

86   After export from the nucleus, pre-miRNAs are processed by Dicer to produce mature 21-24 nt

87   miRNAs that exert their function in the cytoplasm of the cell. In turn, siRNAs are exogenous

88   molecules that may be introduced into the cell either as mature siRNAs or as DNA precursors by

89   transfection or by virus-mediated transduction (Castanotto & Rossi, 2009). Importantly, the

90   degree of complementarity between the small RNA and the target RNA defines the mechanism

91   of posttranscriptional gene silencing: while perfect base complementarity mainly drives target

92   RNA degradation by endonucleolytic cleavage, partial complementarity can lead to translational

93   repression. In animals, the canonical siRNA pathway involves perfect siRNA:target RNA

94   recognition, whereas binding of most miRNAs demands base pairing of the 'seed' region (mostly

95   located at nucleotides 2-8 of the mature miRNA), allowing for imperfect target RNA recognition

96   (reviewed in Carthew & Sontheimer, 2009).

97   The use of RNAi as an antiviral tool has been explored against different viruses (reviewed in

98   Qureshi et al., 2018 and Shah & Schaffer, 2011). Indeed, RNAi mediators such as double-

99   stranded or single-stranded siRNAs and plasmid or virus-encoded short hairpin RNAs (shRNAs)

100   have been evaluated in different experimental settings against animal viruses including FMDV

101   (Chen et al., 2004). Genetically modified animals expressing shRNAs targeting FMDV have also

102   been developed with promising results (Jiao et al., 2013; Hu et al., 2015; Deng et al., 2017). Of

103   note, shRNAs are potent RNAi mediators that usually are expressed at very high levels from

104   RNA-polymerase III promoters; however, this can potentially lead to saturation of the cellular

105   RNAi processing machinery. To overcome this drawback, artificial miRNAs (i.e. miRNAs

106   rationally designed to target defined sequences) have been favored as RNAi shuttles since they

107   exhibit increased safety with comparable efficacy (Boudreau, Martins & Davidson, 2009). The

108   efficacy of artificial miRNAs (amiRNAs) against FMDV has been investigated to a lesser extent

109   (Du et al., 2011; Gismondi et al., 2014; Basagoudanavar et al., 2019). In this work, we further

110   assess the efficacy of amiRNAs against FMDV and shRNAs targeting the same viral regions in

111   susceptible cells.

112

113   **2. Material and methods**

114   2.1 Cells and viruses

115   Baby hamster kidney (BHK-21 clone 13, ATCC CCL10) cells were obtained from the American

116   Type Culture Collection and maintained in Dulbecco's modified Eagle's medium (DMEM, Life

117   Technologies, Grand Island, NY, USA) supplemented with 10% fetal bovine serum (FBS) and

118   antibiotics (Gibco-BRL/Invitrogen, Carlsbad, CA, USA) at 37°C with 5% CO2. Stably

119   transformed cell lines were grown as described in (Gismondi et al., 2014) .

120   FMDV A/Arg/01 isolate A01L (GenBank accession number KY404934) was obtained from the

121   National Institute for Animal Health (SENASA, Argentina). All experiments were conducted

122   using fourth cell passages in BHK-21 cells. Experiments involving active FMDV were

123   performed in the BSL-4 OIE facility at the IVIT (INTA-CONICET; Buenos Aires, Argentina).

124

125   2.2 Plaque assays and virus titration

126   Plaque assays were performed as previously described (Garcia-Nunez et al., 2010). Briefly, cells

127   were infected with serial dilutions of virus and incubated for 48 h at 37°C with 5% CO_2.

128   Monolayers were fixed with 4% formaldehyde and stained with crystal violet, and the number

129   and area of individual plaques (n $\geq$ 18) were determined by using ViralPlaque (Cacciabue, Curra

130   & Gismondi, 2019). Assays were performed in duplicate.

131 Virus titers were determined in BHK-21 cells as described in (Gismondi et al., 2014) .

132

133 2.3 Prediction of RNAi target sequences

134 Target sequences within FMDV 3Dpol coding region (nucleotides 6681-8093 of FMDV A01L)

135 were predicted with RNAxs software (Tafer et al., 2008). This program is freely available at

136 http://rna.tbi.univie.ac.at/cgi-bin/RNAxs/RNAxs.cg. It relies on several siRNA design criteria,

137 namely siRNA strand selection (using both sequence and energy-based rules), self-folding (the

138 minimal free folding-energy of the guide strand), free-end (number of paired nucleotides among

139 the first four at the 5' end and the 3'end of the guide strand) and most importantly accessibility

140 (probability that a region of predefined length is free of base pairing in thermodynamic

141 equilibrium). The program (accessed by October 2014) was run with default values for siRNA.

142 The output file of RNAxs includes a number of putative target sequences of 19 nt. To adapt the

143 prediction software to 21 nt target sequences, 2 additional nucleotides were incorporated to each

144 designed small RNA (see Results). Lastly, small RNAs targeting 3Dpol sequence 1162-1182

145 were also used since this region showed high flexibility in a local SHAPE-directed RNA

146 structure obtained at our laboratory (Supplementary Figure 1 and unpublished results).

147 Moreover, it was previously demonstrated that this stretch of FMDV O/CHA/99 can be

148 successfully targeted by RNAi (Gu et al., 2014). In addition, a plasmid encoding a control

149 sequence not expected to target any mammalian mRNA, EGFP or FMDV was used as a negative

150 control.

151

152 2.4 Plasmids

153   2.4.1 shRNA encoding plasmids

154   RNA polymerase III U6 promoter including a BbsI site at the 3' end was amplified by PCR and

155   cloned within plasmid TOPO pCR2.1 (Invitrogen, Carlsbad, USA) to create plasmid pTOPO-U6.

156   Complementary single-stranded DNA oligonucleotides encoding shRNA against predicted target

157   sequences (Table 1; Supplementary Table 1) were synthesized (Macrogen, Seoul, Korea),

158   annealed and cloned into the BbsI restriction site in pTOPO-U6. The resulting plasmids were

159   named pshRNA$_{FMDV}$, where FMDV is the target sequence ID.

160   2.4.2 Pre-amiRNA encoding plasmids

161   Individual pre-amiRNA coding sequences were cloned into into pcDNA®6.2-GW/miR vector

162   (BLOCK-iT Pol II miR RNAi expression vector kit, Invitrogen, Carlsbad, USA) as described in

163   (Gismondi et al., 2014) . The resulting plasmids were named pamiRNA$_{FMDV}$, where FMDV is

164   the target sequence ID.

165   Dual amiRNA$_{FMDV}$-expressing plasmids were assembled from individual pamiRNA$_{FMDV}$

166   according to the manufacturer's instructions (BLOCK-iT Pol II miR RNAi expression vector kit,

167   Invitrogen, Carlsbad, USA) Briefly, donor pamiRNA$_{FMDV}$ DNA was digested with BamHI and

168   XhoI and the purified pre-amiRNA$_{FMDV}$ encoding sequence was subcloned into acceptor

169   pamiRNA$_{FMDV}$ previously digested with BglII and XhoI enzymes.

170

171   2.4.3 Enhanced green fluorescent protein (EGFP) reporter plasmids

172   A reporter plasmid encoding the EGFP gene fused to the complete FMDV 3Dpol-coding

173   sequence (pEGFP.3D) was constructed. To this end, the EGFP coding sequence was amplified

174   by PCR using oligonucleotides EGFPfor and EGFPrev (Supplementary Table 1) and cloned

175   between KpnI and EcoRI restriction sites in pcDNA3 vector (Invitrogen, Carlsbad, USA). In

176   addition, the FMDV A01L 3Dpol-coding sequence was amplified by PCR and cloned

177   immediately downstream of the EGFP termination codon.

178   All recombinant vectors were confirmed by automated sequencing.

179

180   2.5 Transfection and electroporation

181   Pre-amiRNA$_{FMDV}$ and shRNA$_{FMDV}$-encoding plasmids were transfected into 95% confluent

182   BHK-21 cells seeded in 48-well culture plates using PolyAr reagent (School of Biochemistry and

183   Pharmacy, University of Buenos Aires), according to manufacturer's instructions. Briefly, cells

184   were washed with serum-free DMEM, and incubated with 125 µl of transfection mixture

185   containing 900 ng DNA, 1 µl PolyAr and DMEM for 4 h at 37ºC and 5% CO_2. Transfected cells

186   were washed three times with sterile 1X PBS and incubated for additional time in DMEM

187   10% FBS at 37ºC and 5% CO_2.

188   When indicated, $1.3×10^6$ BHK-21 cells were electroporated with 6 µg DNA using GenePulser

189   XCell (BioRad, Hercules, CA, USA). Electroporation conditions included 1 pulse at 280 V for

190   25 ms in 4mm-cuvettes. Electroporated cells were seeded in 48-well culture plates and incubated

191   in DMEM 10% FBS at 37ºC and 5% CO_2 for 18 h prior to FMDV infection.

192

193   2.6 Reporter assays

194   Plasmid pEGFP.3D was co-transfected with either pshRNA$_{FMDV}$ or pamiRNA$_{FMDV}$ at a 1:3 molar

195   ratio using PolyAr as described above. At 24 h postransfection, EGFP expression was evaluated

196   by fluorescence microscopy in a Zeiss microscope. In addition, transfected cells were washed 2

197   times with 1X PBS, trypsinized and fixed in 1% formaldehyde for 20 min on ice. After 2 washes

198   in 1X PBS 2mM EDTA, EGFP expression was quantified by flow cytometry. A BD

199   FACSCalibur and FlowJo™ Software (Becton, Dickinson and Company; 2019) were used to

200   measure frequency and median fluorescence intensity of EGFP+ cells. Of the 10,000 events

201   evaluated per sample, only those with the forward scatter and side scatter properties of viable

202   cells were used in measurements of EGFP fluorescence intensity.

203

204   2.7 Establishment of transgenic cell lines

205   At 24 h post-transfection with pamiRNA$_{FMDV}$, cells were subcultured in DMEM medium

206   containing 10% FBS and 7 µg/ml blasticidin S (Invitrogen, Carlsbad, USA). Transgenic

207   polyclonal cell lines were established by consecutive passages in DMEM 10% FBS and 7 µg/ml

208   blasticidin S.

209   Polyclonal cell lines were further cloned by limiting dilution as described in (Gismondi et al.,

210   2014). Transgenesis was confirmed by PCR using oligonucleotides miRNAseq for and

211   miRNAseq rev (Supplementary Table 1).

212

213   2.8 Antiviral activity of small RNAs against FMDV

214   Electroporated cells were infected for 60 min at a multiplicity of infection (moi) of 3-5. Cells

215   were washed with 1X PBS pH 5.0 on ice to inactivate unabsorbed virus. After restitution of

216   physiological pH, cells were incubated in DMEM 2% FBS and 25 mM HEPES pH 7.5 at 37 °C

217   in a 5% CO_2 atmosphere. At indicated times post-infection, cells were lysed by three consecutive

218   freeze-thaw cycles and the amount of viral particles was measured by the $TCID_{50}$ method as

219   mentioned above. Percentage of inhibition was calculated from the following equation: P = ((A-

220   B)*100)/A, where A was viral titer of cell lines expressing miRneg infected with FMDV

221   A/Arg/01, and B was viral titer of cell lines expressing $amiRNA_{FMDV}$ infected with FMDV

222   A/Arg/01. Experiments were performed in duplicate.

223   Stable cell lines expressing $amiRNA_{FMDV}$ were infected at an moi of 0.001 and incubated in

224   DMEM 2% FBS and 25 mM HEPES pH 7.5 at 37 °C and 5% CO_2. At different times post-

225   infection, the virus present in supernatants was titrated by the $TCID_{50}$ method.

226

227   2.9 Statistical analysis

228   Student's t test was used to compare mean viral titers in different samples and mean plaque areas.

229   Differences in median fluorescence intensity in cells transfected with different plasmids were

230   compared using Kruskal-Wallis test. A p value <0.05 was considered as statistically significant.

231

232   **3. Results**

233   3.1 Selection of target sequences

234 Target sequences were predicted within FMDV A01L 3Dpol-coding sequence with RNAxs

235 software (Tafer et al., 2008), which applies several prediction parameters including RNA

236 accessibility. A total number of 178 target sequences were predicted along 3D (Figure 1, blue

237 areas; Supplementary Table 2), with top 50 predicted targets concentrated in discrete regions

238 (Figure 1, red areas).

239 Next, an additional screening of the target sequences ranking in the top positions of the RNAxs

240 output was performed to take into account the prediction rules proposed by Low et al. (Low et

241 al., 2012). Firstly, 19 nt target sequences were extended to 21 nt in order to adapt RNAxs

242 prediction to amiRNA-compatible length. Then, the resulting target sequences were analyzed in

243 terms of the accessibility window proposed by Low et al., i.e., sequences showing a less

244 structured stretch downstream of the 21 nt target region were favored. Lastly, the total free

245 energy change (ΔGtotal) of target:siRNA duplex formation was calculated with OligoWalk

246 program (Reuter & Mathews, 2010) (Table 1). After applying these rules, sequences 444-464,

247 290-310 and 1055-1075 were selected (termed 444; 290 and 1055; Figure 1, Table 1 and

248 Supplementary Figure 1). The selected target sequences ranked in the first positions of the

249 RNAxs output. Indeed, in some cases the 21 nt target sequences included more than one 19 nt

250 predicted target sequence (Table 1). Of note, sequences 290 and 444 displayed a ΔGtotal value

251 higher than the one recommended by Low et al. (-25 Kcal/mol). Regarding the accessibility

252 window, no target sequence showed the expected accessible 13 nt window starting at position 14

253 (Supplementary Figure 1a). However, all sequences were located in the region of high linear

254 correlation between RNA structure and shRNA efficacy described by these authors

255 (Supplementary Figure 1B).

256   Finally, conservation of the selected target sequences among prototypic strains of the South

257   American serotype pool was evaluated (Supplementary Figure 1C). Sequences 290, 444 and

258   1055 showed some polymorphisms between serotypes, which were distributed mainly outside

259   the seed region.

260

261   3.2 Silencing efficacy of shRNAs and amiRNAs targeting selected FMDV sequences

262   A reporter assay was conducted to test the silencing efficacy of different RNAi mediators

263   targeting the selected sequences. To this end, a plasmid encoding EGFP fused to the 3Dpol-

264   coding sequence of FMDV A/Arg/01 was co-transfected with plasmids encoding either shRNAs

265   or amiRNAs targeting each individual FMDV sequence. Short hairpin RNAs targeting sequences

266   290, 444 and 1055 induced a significant reduction of EGFP expression in co-transfected cells, as

267   determined by fluorescence microscopy and flow cytometry (Figure 2A and Supplementary

268   Figure 2A). In turn, amiRNAs targeting single FMDV sequences also exhibited significant

269   silencing activity (Figure 2B and Supplementary Figure 2B).

270   To evaluate the impact of dual amiRNA$_{FMDV}$ expression on silencing activity in reporter assays,

271   pre-amiRNA$_{290}$, pre-amiRNA$_{444}$ or pre-amiRNA$_{1162}$ were subcloned in pamiRNA$_{1055}$ to obtain

272   bicistronic expression constructs and the resulting plasmids were co-transfected with pEGFP.3D

273   in BHK-21 cells. As shown in Figure 2C, dual expression of amiRNAs did not enhance silencing

274   of the reporter mRNA.

275

276   3.3 Antiviral activity of shRNA$_{FMDV}$ and amiRNA$_{FMDV}$

277   Next, we evaluated the antiviral activity of shRNAs and amiRNAs against FMDV in cultured

278   cells. To this end, BHK-21 cells were electroporated with the small RNA-expressing plasmids,

279   and after 16 h the cells were infected with FMDV at high multiplicity of infection. Viral titers

280   were determined at different times post infection to assess the effect of small RNAs on viral

281   growth. As listed in Table 2, inhibition of viral growth was evidenced at 5 hours post-infection

282   (hpi) in cells expressing small RNAs targeting regions 290, 444 and 1055. Interestingly,

283   shRNA$_{290}$ induced a 2-fold reduction of FMDV replication, whereas shRNA$_{444}$ and shRNA$_{1055}$

284   induced a more pronounced decrease in viral titers at this time point. Conversely, there was a

285   higher inhibition of viral growth in cells expressing amiRNA$_{290}$ (>10-fold) than in cells

286   electroporated with pamiRNA$_{444}$ and pamiRNA$_{1055}$. Again, dual expression of amiRNAs

287   targeting different FMDV sequences did not improve the silencing activity of each individual

288   amiRNA (Table 2). Of note, the silencing efficacy of small RNAs determined previously in our

289   reporter assays was confirmed in the context of viral replication except for shRNA$_{1162}$, which did

290   not affect FMDV replication significantly.

291

292   3.4 Stable expression of amiRNAs against FMDV

293   Electroporation of DNA is a well-established method that yields a high frequency of

294   transformants (Potter, 2003); however, transfection efficiency is not 100%. We hypothesized that

295   electroporation of plasmids expressing small RNAs could lead to a population of non-transfected

296   cells that, when infected, would contribute to FMDV replication. To circumvent this possibility,

297   stably-transformed cell lines expressing amiRNA$_{290}$ and amiRNA$_{1055}$ were established and

298 characterized in terms of antiviral efficacy. In this case, only amiRNAs were evaluated since

299 they exhibit less toxicity than shRNAs (Boudreau, Monteys & Davidson, 2008).

300 Pre-amiRNA$_{FMDV}$ expressing plasmids were stably transfected in BHK-21 cells and transgenic

301 polyclonal cell lines were selected by blasticidin resistance. Mature amiRNA expression was

302 confirmed by RT-stem loop qPCR (Supplementary Figure 4A). After several passages, cells

303 were infected with FMDV A/Arg/01 and cultures were monitored to evaluate the development of

304 cytopathic effect. At 48 hpi, control cell monolayers (non-transfected BHK-21 cells and cells

305 stably transfected with a non-specific amiRNA) were completely detached due to FMDV

306 infection. In contrast, infection of cell lines stably expressing amiRNA$_{290}$ and amiRNA$_{1055}$

307 caused partial cytopathic effect, with a significant proportion of cells still adherent to the culture

308 surface (Figure 3A). This effect was also evidenced in lysis plaques assays, where FMDV

309 infection rendered less plaques of smaller dimensions in cell lines expressing amiRNA$_{290}$ and

310 amiRNA$_{1055}$ than in control cells (Figure 3B). However, viral titers determined at different times

311 post-infection in supernatants of amiRNA$_{290}$ and amiRNA$_{1055}$ polyclonal cells did not differ

312 significantly from control cells except for amiRNA$_{290}$ cells at 18 hpi (Figure 3C). Together, these

313 results suggest a transient amiRNA-mediated constraint on FMDV replication in transgenic cell

314 lines.

315 Next, polyclonal cell lines expressing amiRNA$_{290}$ and amiRNA$_{1055}$ were cloned by limiting

316 dilution to consider the potential variability in transgene expression associated with multiple

317 transgene insertion events during the establishment and selection of stable transformants. The

318 resulting cell lines were infected with FMDV A/Arg/01 and their ability to control viral growth

319 was assessed by plaque assay (data not shown). Cloned cell lines showing less or smaller plaques

320 than control cells (BHK-21 and miRneg-expressing cells) were selected for further analysis.

321 Selected cell lines (n=4 for amiRNA$_{290}$ and n=3 for amiRNA$_{1055}$) were infected with FMDV

322 A/Arg/01 and viral growth was determined by viral titration in supernatants at different times

323 post-infection. As shown in Figure 4, viral growth was delayed in the majority of the cloned cell

324 lines, supporting the potential use of amiRNAs as antivirals. However, at 48 hpi, the viral titers

325 in supernatants of infected transgenic cells did not differ from control cells. Moreover, direct

326 sequencing of a 250-300 nt region encompassing the target site did not show any mutation that

327 could account for virus escape (Supplementary Figure 5).

328

329 ## 4. Discussion

330 To develop an antiviral strategy against FMDV based on RNAi, the 3Dpol-coding sequence of

331 FMDV A/Arg/01 was used to predict target sites. This region of the viral genome is highly

332 conserved within FMDV serotypes. Moreover, the essential role played by the protein product

333 (3Dpol) in the viral replication cycle makes it an attractive target for RNA interference. As

334 shown in the reporter assays, the predicted targets were silenced efficiently independently of the

335 RNAi mediator used, supporting the feasibility of the algorithm applied for target selection. Our

336 results are in accordance with previous data indicating that the 3D region of the FMDV genome

337 is a suitable target for RNAi (Pengyan et al., 2008; Du et al., 2011; Gu et al., 2014;

338 Basagoudanavar et al., 2019) and they represent a step forward in the identification of new target

339 sequences within FMDV, specifically in serotype A, that had been less explored in previous

340 works.

341 It is well known that target accessibility may limit RNAi efficacy (Westerhout, 2005; Tafer et al.,

342 2008; Low et al., 2012; Gismondi et al., 2014). In a paper on HIV inhibition by RNAi, Low et al.

343   (2012) analyzed the impact of target RNA structure and target:siRNA duplex thermodynamics

344   on shRNA efficacy. They found a maximal negative correlation for a 13-nt window that starts at

345   position 14 of the target RNA and extends over 7 nucleotides downstream of the "seed region"

346   binding site. In the context of RNAi, a negative correlation implies that maximal shRNA

347   inhibition is achieved for less structured target RNAs. Moreover, ΔGtotal of target:siRNA duplex

348   formation strongly correlated with shRNA inhibition. Thus, in this work RNA accessibility was

349   used as a central criterion for target selection.

350   The available programs for prediction of RNAi targets can be classified as first- and second-

351   generation algorithms. The latter are based not only on a number of selection criteria but also

352   they were optimized to include results from real RNAi experiments to validate their predictions

353   (Griger & Tisminetzky, 1984; Devaney et al., 1988; Filhol et al., 2012). In the present work we

354   used a first-generation RNAi target selection program but we also included the experimental data

355   derived from the work by Low et al (2012) to predict RNAi targets. Interestingly, none of the

356   selected regions had been targeted previously in other similar studies with other FMDV

357   serotypes (Chen et al., 2004; Kahana et al., 2004; Mohapatra et al., 2005; Du et al., 2011).

358   Furthermore, our analysis with RNAxs did not retrieve the targets selected by other authors

359   within the 15 best ranking sequences or it did even not predict them at all. This may indicate

360   that, despite sequence conservation between FMDV serotypes in the 3D region, accessibility of

361   specific target sequences may not be equivalent between serotypes due to structural constraints

362   in the context of the whole genome, as we previously reported.

363   Indeed, conservation of the target sequence among different viral strains should be considered

364   during the development of RNAi-based antiviral tools (Mcintyre et al., 2009). In this work,

365   selected sequences 290, 444 and 1055 showed partial conservation among South American

366   serotypes; however, the sequences used for small RNA design were the most frequent at

367   polymorphic sites (Supplementary Figure 1C). Interestingly, other stretches within 3D showing

368   100% conservation were not predicted in the top-ranking target sites by RNAxs software,

369   suggesting these sequences may not be accessible. Initial reports on determinants of

370   miRNA:mRNA recognition highlighted the existence of two categories of target sites. 5'

371   dominant sites, which are strongly complementary to the miRNA 5' end, need little or no pairing

372   of the miRNA 3' end to achieve silencing. On the other hand, miRNAs with partial

373   complementarity at the 5' end require strong 3' compensatory pairing for function (Brennecke et

374   al., 2005; Bartel, 2009). Thus, the existence of polymorphisms in the target sequence should not

375   preclude miRNA efficacy against different FMDV serotypes. Moreover, potentially reduced

376   RNAi due to weak amiRNA:target RNA pairing at polymorphic sites could be circumvented by

377   co-expression of multiple amiRNAs targeting different target sequences of the viral genome.

378   Interestingly, the shRNA directed against sequence 1162 was effective in the reporter assay and

379   the amiRNA trended to perform in a similar way, although with no statistical significance.

380   Contrarily, $shRNA_{1162}$ did not affect FMDV replication significantly, whereas $amiRNA_{1162}$

381   showed moderate antiviral activity. This target region was selected as a putative positive control,

382   since the same sequence of FMDV serotype O/CHA/99 (Supplementary Figure 3) had been

383   efficiently silenced by an shRNA in a previous paper (Gu et al., 2014). Noteworthy, as

384   mentioned before, this region was not predicted as a suitable RNAi target by RNAxs software. It

385   may be argued that $shRNA_{1162}$ did not work due to structural constraints of the target region in

386   the context of the whole viral genome, which were not present in the reporter mRNA. However,

387   the results obtained with $amiRNA_{1162}$ indicate that target site accessibility should not be limiting

388    $shRNA_{1162}$ efficacy. Alternatively, it is possible that this target region is not completely

389 accessible to the mature small RNAs, leaving only some nucleotides available for small

390 RNA:target recognition. In this case, pairing of the seed region of $amiR_{1162}$ would be sufficient

391 for activation of the RNAi machinery, whereas incomplete pairing between $shRNA_{1162}$ and its

392 target RNA would not lead to RNA silencing. In addition, since it has been shown that siRNA

393 derived from shRNA precursors are more heterogeneous in cleavage sites and length than small

394 RNAs originating from miRNA precursors (Maczuga et al., 2013), differences in shRNA and

395 pre-amiRNA structures and processing that may lead to slightly different mature small RNAs

396 with singular silencing efficacy cannot be ruled out.

397 Short hairpin RNAs are highly transcribed from RNA polymerase III promoters such as the U6

398 promoter used in this study. In addition, it has been demonstrated that shRNAs are more potent

399 than amiRNAs (Boudreau, Monteys & Davidson, 2008) when they are expressed from the same

400 promoter. However, shRNAs exhibit higher cellular toxicity than amiRNAs since the high levels

401 of shRNA precursors produced in a cell may saturate the endogenous miRNA processing

402 machinery (Boudreau, Martins & Davidson, 2009). In our reporter assays, shRNAs and

403 amiRNAs were transcribed from different promoters (U6 and CMV, for RNA polymerases III

404 and II, respectively). and we did not detect any difference in cell viability between cells

405 transfected with $pshRNA_{FMDV}$ and cells transfected with $pamiRNA_{FMDV}$ as determined by flow

406 cytometry.

407 Our results show that amiRNAs induce a significant inhibition of viral replication in cultured

408 cells; however, silencing of FMDV RNA is not complete leading to sustained viral replication.

409 Notably, amiRNAs were poorly expressed in the majority of cloned cell lines as compared to

410 polyclonal cells (Supplementary Figure 4B). Thus, the lack of sustained viral inhibition may be

411 associated with insufficient amiRNA expression. However, a ~24 h delay in viral replication has

412   been also reported by de los Santos et al (de los Santos et al., 2005), Chen et al (Chen et al.,

413   2004) and Lv et al (Lv et al., 2009) using shRNAs or siRNAs. Conversely, Kahana et al (Kahana

414   et al., 2004) showed a sustained inhibition of FMDV infection in BHK-21 cells transfected with

415   siRNAs against FMDV; however, the authors only analyzed viral replication for 24 h. In turn, by

416   using an siRNA transfected in BHK-21 cells, Mohapatra et al (Mohapatra et al., 2005) reported a

417   reduction of viral titer of >99% at 24 hpi and >87% at 48 hpi. The transitory character of viral

418   inhibition may be explained by several factors. First of all, it should be kept in mind that in the

419   infected cell the FMDV RNA is associated with multiple cellular and viral proteins during the

420   processes of genome translation and replication. Thus, target sequences should not be expected

421   to be continuously accessible for the silencing complexes during the whole FMDV replication

422   cycle. In addition, it is well known that FMDV proteases induce a rapid shut-off of cellular

423   transcription and cap-dependent translation (Kim et al., 2008; Qureshi, Thakur & Kumar, 2013).

424   Given that amiRNAs are expressed from the strong CMV promoter, it is expected that pre-

425   amiRNA transcription is also inhibited in infected cells in the context of viral replication. Thus,

426   the incomplete inhibition of FMDV replication by amiRNAs may be explained by a FMDV-

427   mediated reduction in transgene expression.

428   Other authors have demonstrated that simultaneous expression of multiple small RNAs directed

429   against different regions of the same target RNA can increase silencing efficacy (Kahana et al.,

430   2004; Brake et al., 2008; Liu et al., 2008; Kim et al., 2010; Saha et al., 2016). This approach

431   becomes particularly relevant when the target RNA is a viral genome, since multiple small

432   RNAs acting on the same genome reduce the chance of emergence of escape mutants thus

433   increasing safety. However, in this work dual amiRNA expression did not enhance silencing of

434   the reporter mRNA or the complete FMDV genome as compared to individual amiRNA

435   expression. Similar results have been reported by other authors using amiRNAs against FMDV

436   (Basagoudanavar et al., 2019). Noteworthy, amiRNA expression did not differ significantly in

437   cells stably transfected with monocistronic or bicistronic vectors (Supplementary Figure 4A).

438   Further research is needed to determine whether it is due to structural constraints of the target

439   RNA or to the intrinsic regulation of the RNAi machinery.

440

5. Conclusions

442   In light of the results obtained, we conclude that the selection algorithm proved to be highly

443   accurate in the identification of target sequences. FMDV replication may be transiently

444   controlled by amiRNAs targeting 3D. Ongoing work in our laboratory is aimed at finding new

445   targets in other genomic regions of FMDV to develop additional amiRNAs that could potentiate

446   the antiviral effects observed in the present work. Our results highlight the potential application

447   of amiRNAs as antiviral tools which may complement vaccination, specifically to prevent the

448   spread of the disease during outbreaks in endemic or non-endemic countries.

449

Acknowledgements

451   A.C. is a doctoral fellow and M.C of the National Research Council (CONICET) at the

452   University of Luján, Argentina. M.C. is a postdoctoral fellow of CONICET. S.A., O.T. and

453   M.I.G. are members of CONICET Research Career Program.

454 We thank María José Mónaco and Osvaldo Zábal for technical assistance and Juan Manuel

455 Schammas and Alfredo Perea for their support during our work in the BSL4-OIE facilities at the

456 Institute of Virology–INTA.

457

458

459 **References**

460 Andino R, Domingo E. 2015. Viral quasispecies. *Virology* 479–480:46–51. DOI:

461   10.1016/j.virol.2015.03.022.

462 Bartel DP. 2009. MicroRNAs: Target Recognition and Regulatory Functions. *Cell* 136:215–233.

463   DOI: 10.1016/j.cell.2009.01.002.

464 Basagoudanavar SH, Ranjitha HB, Hosamani M, Kolangath SM, Selvan RPT, Sreenivasa BP,

465   Saravanan P, Sanyal A, Venkataramanan R. 2019. Efficient inhibition of foot-and-mouth

466   disease virus replication in vitro by artificial microRNA targeting 3D polymerase. *Acta*

467   *Virol* 63:475–479. DOI: 10.4149/av_2019_407.

468 Boudreau RL, Martins I, Davidson BL. 2009. Artificial microRNAs as siRNA shuttles: improved

469   safety as compared to shRNAs in vitro and in vivo. *Mol Ther* 17:169–75. DOI:

470   10.1038/mt.2008.231.

471 Boudreau RL, Monteys AM, Davidson BL. 2008. Minimizing variables among hairpin-based

472   RNAi vectors reveals the potency of shRNAs. *RNA* 14:1834–44. DOI:

473   10.1261/rna.1062908.

474 Brake O ter, Hooft K 't, Liu YP, Centlivre M, Jasmijn von Eije K, Berkhout B. 2008. Lentiviral

475   Vector Design for Multiple shRNA Expression and Durable HIV-1 Inhibition. *Molecular*

476   *Therapy* 16:557–564. DOI: 10.1038/sj.mt.6300382.

477   Brennecke J, Stark A, Russell RB, Cohen SM. 2005. Principles of MicroRNA–Target

478   Recognition. *PLoS Biology* 3:e85. DOI: 10.1371/journal.pbio.0030085.

479   Cacciabue M, Curra A, Gismondi MI. 2019. ViralPlaque: a Fiji macro for automated assessment

480   of viral plaque statistics. *PeerJ* 7:e7729. DOI: 10.7717/peerj.7729.

481   Carthew RW, Sontheimer EJ. 2009. Origins and Mechanisms of miRNAs and siRNAs. *Cell*

482   136:642–55. DOI: 10.1016/j.cell.2009.01.035.

483   Castanotto D, Rossi JJ. 2009. The promises and pitfalls of RNA-interference-based therapeutics.

484   *Nature* 457:426–33. DOI: 10.1038/nature07758.

485   Chen C. 2005. Real-time quantification of microRNAs by stem-loop RT-PCR. *Nucleic Acids*

486   *Research* 33:e179–e179. DOI: 10.1093/nar/gni178.

487   Chen W, Yan W, Du Q, Fei L, Liu M, Ni Z, Sheng Z, Zheng Z. 2004. RNA interference

488   targeting VP1 inhibits foot-and-mouth disease virus replication in BHK-21 cells and

489   suckling mice. *J Virol* 78:6900–7. DOI: 10.1128/JVI.78.13.6900-6907.2004.

490   Deng S, Li G, Yu K, Tian X, Wang F, Li W, Jiang W, Ji P, Han H, Fu J, Zhang X, Zhang J, Liu

491   Y, Lian Z, Liu G. 2017. RNAi combining Sleeping Beauty transposon system inhibits ex

492   vivo expression of foot-and-mouth disease virus VP1 in transgenic sheep cells. *Sci Rep*

493   7:10065. DOI: 10.1038/s41598-017-09302-1.

494   Devaney MA, Vakharia VN, Lloyd RE, Ehrenfeld E, Grubman MJ. 1988. Leader protein of foot-

495   and-mouth disease virus is required for cleavage of the p220 component of the cap-

496   binding protein complex. *J Virol* 62:4407–9.

497   Dicara D, Burman A, Clark S, Berryman S, Howard MJ, Hart IR, Marshall JF, Jackson T. 2008.

498   Foot-and-mouth disease virus forms a highly stable, EDTA-resistant complex with its

499   principal receptor, integrin alphavbeta6: implications for infectiousness. *J Virol* 82:1537–

500   46. DOI: 10.1128/JVI.01480-07.

501 Domingo E, Escarmı́s C, Baranowski E, Ruiz-Jarabo CM, Carrillo E, Núñez JI, Sobrino F. 2003.

502   Evolution of foot-and-mouth disease virus. *Virus Research* 91:47–63. DOI:

503   10.1016/s0168-1702(02)00259-9.

504 Domingo E, Sheldon J, Perales C. 2012. Viral Quasispecies Evolution. *Microbiology and*

505   *Molecular Biology Reviews* 76:159–216. DOI: 10.1128/MMBR.05023-11.

506 Du J, Gao S, Luo J, Zhang G, Cong G, Shao J, Lin T, Cai X, Chang H. 2011. Effective inhibition

507   of foot-and-mouth disease virus (FMDV) replication in vitro by vector-delivered

508   microRNAs targeting the 3D gene. *Virol J* 8:292. DOI: 10.1186/1743-422X-8-292.

509 Filhol O, Ciais D, Lajaunie C, Charbonnier P, Foveau N, Vert JP, Vandenbrouck Y. 2012. DSIR:

510   assessing the design of highly potent siRNA by testing a set of cancer-relevant target

511   genes. *PLoS One* 7:e48057. DOI: 10.1371/journal.pone.0048057.

512 Fischer SEJ. 2015. RNA Interference and MicroRNA-Mediated Silencing. *Curr Protoc Mol Biol*

513   112:26 1 1-26 1 5. DOI: 10.1002/0471142727.mb2601s112.

514 Garcia-Nunez S, Konig G, Berinstein A, Carrillo E. 2010. Differences in the virulence of two

515   strains of Foot-and-Mouth Disease Virus Serotype A with the same spatiotemporal

516   distribution. *Virus Res* 147:149–52. DOI: 10.1016/j.virusres.2009.10.013.

517 Gismondi MI, Ortiz XP, Curra AP, Asurmendi S, Taboga O. 2014. Artificial microRNAs as

518   antiviral strategy to FMDV: structural implications of target selection. *J Virol Methods*

519   199:1–10. DOI: 10.1016/j.jviromet.2013.12.016.

520 Golde W, Pacheco J, Duque H, Doel T, Penfold B, Ferman G, Gregg D, Rodriguez L. 2005.

521   Vaccination against foot-and-mouth disease virus confers complete clinical protection in

522   7 days and partial protection in 4 days: Use in emergency outbreak response. *Vaccine*

523   23:5775–5782. DOI: 10.1016/j.vaccine.2005.07.043.

524   Griger PR, Tisminetzky SG. 1984. Histone H3 modification in BHK cells infected with foot-and-

525   mouth disease virus. *Virology* 136:10–19. DOI: 10.1016/0042-6822(84)90243-5.

526   Grubman MJ, Baxt B. 2004. Foot-and-mouth disease. *Clin Microbiol Rev* 17:465–93. DOI:

527   10.1128/cmr.17.2.465-493.2004.

528   Gu YX, Gao ZL, Zhou JH, Zhang J, Liu YS. 2014. Establishment and evaluation of stable cell

529   lines inhibiting foot-and-mouth disease virus by RNA interference. *Biomed Res Int*

530   2014:109428. DOI: 10.1155/2014/109428.

531   Hu S, Qiao J, Fu Q, Chen C, Ni W, Wujiafu S, Ma S, Zhang H, Sheng J, Wang P, Wang D,

532   Huang J, Cao L, Ouyang H. 2015. Transgenic shRNA pigs reduce susceptibility to foot

533   and mouth disease virus infection. *Elife* 4:e06951. DOI: 10.7554/eLife.06951.

534   Jiao Y, Gong X, Du J, Liu M, Guo X, Chen L, Miao W, Jin T, Chang H, Zeng Y, Zheng Z. 2013.

535   Transgenically mediated shRNAs targeting conserved regions of foot-and-mouth disease

536   virus provide heritable resistance in porcine cell lines and suckling mice. *Vet Res* 44:47.

537   DOI: 10.1186/1297-9716-44-47.

538   Kahana R, Kuznetzova L, Rogel A, Shemesh M, Hai D, Yadin H, Stram Y. 2004. Inhibition of

539   foot-and-mouth disease virus replication by small interfering RNA. *J Gen Virol* 85:3213–

540   3217. DOI: 10.1099/vir.0.80133-0.

541   Kim SM, Lee KN, Lee SJ, Ko YJ, Lee HS, Kweon CH, Kim HS, Park JH. 2010. Multiple

542   shRNAs driven by U6 and CMV promoter enhances efficiency of antiviral effects against

543   foot-and-mouth disease virus. *Antiviral Res* 87:307–17. DOI:

544   10.1016/j.antiviral.2010.06.004.

545 Kim SM, Lee KN, Park JY, Ko YJ, Joo YS, Kim HS, Park JH. 2008. Therapeutic application of
546   RNA interference against foot-and-mouth disease virus in vitro and in vivo. *Antiviral Res*
547   80:178–84. DOI: 10.1016/j.antiviral.2008.06.001.

548 Lawrence P, Rai D, Conderino JS, Uddowla S, Rieder E. 2016. Role of Jumonji C-domain
549   containing protein 6 (JMJD6) in infectivity of foot-and-mouth disease virus. *Virology*
550   492:38–52. DOI: 10.1016/j.virol.2016.02.005.

551 Liu YP, Haasnoot J, ter Brake O, Berkhout B, Konstantinova P. 2008. Inhibition of HIV-1 by
552   multiple siRNAs expressed from a single microRNA polycistron. *Nucleic Acids Res*
553   36:2811–24. DOI: 10.1093/nar/gkn109.

554 Low JT, Knoepfel SA, Watts JM, ter Brake O, Berkhout B, Weeks KM. 2012. SHAPE-directed
555   discovery of potent shRNA inhibitors of HIV-1. *Mol Ther* 20:820–8. DOI:
556   10.1038/mt.2011.299.

557 Lv K, Guo Y, Zhang Y, Wang K, Li K, Zhu Y, Sun S. 2009. Transient inhibition of foot-and-
558   mouth disease virus replication by siRNAs silencing VP1 protein coding region. *Res Vet*
559   *Sci* 86:443–52. DOI: 10.1016/j.rvsc.2008.10.011.

560 Maczuga P, Lubelski J, van Logtenstein R, Borel F, Blits B, Fakkert E, Costessi A, Butler D, van
561   Deventer S, Petry H, Koornneef A, Konstantinova P. 2013. Embedding siRNA sequences
562   targeting apolipoprotein B100 in shRNA and miRNA scaffolds results in differential
563   processing and in vivo efficacy. *Mol Ther* 21:217–27. DOI: 10.1038/mt.2012.160.

564 Mcintyre GJ, Groneman JL, Yu Y-H, Jaramillo A, Shen S, Applegate TL. 2009. 96 shRNAs
565   designed for maximal coverage of HIV-1 variants. *Retrovirology* 6:55. DOI:
566   10.1186/1742-4690-6-55.

567   Mohapatra JK, Sanyal A, Hemadri D, Tosh C, Kumar RM, Bandyopadhyay SK. 2005.

568   Evaluation of in vitro inhibitory potential of small interfering RNAs directed against

569   various regions of foot-and-mouth disease virus genome. *Biochem Biophys Res Commun*

570   329:1133–8. DOI: 10.1016/j.bbrc.2005.02.080.

571   Pengyan W, Yan R, Zhiru G, Chuangfu C. 2008. Inhibition of foot-and-mouth disease virus

572   replication in vitro and in vivo by small interfering RNA. *Virol J* 5:86. DOI:

573   10.1186/1743-422X-5-86.

574   Potter H. 2003. Transfection by electroporation. *Curr Protoc Mol Biol* Chapter 9:Unit 9 3. DOI:

575   10.1002/0471142727.mb0903s62.

576   Qureshi A, Tantray VG, Kirmani AR, Ahangar AG. 2018. A review on current status of antiviral

577   siRNA. *Rev Med Virol* 28:e1976. DOI: 10.1002/rmv.1976.

578   Qureshi A, Thakur N, Kumar M. 2013. VIRsiRNApred: a web server for predicting inhibition

579   efficacy of siRNAs targeting human viruses. *J Transl Med* 11:305. DOI: 10.1186/1479-

580   5876-11-305.

581   Reuter JS, Mathews DH. 2010. RNAstructure: software for RNA secondary structure prediction

582   and analysis. *BMC Bioinformatics* 11:129. DOI: 10.1186/1471-2105-11-129.

583   Saha A, Bhagyawant SS, Parida M, Dash PK. 2016. Vector-delivered artificial miRNA

584   effectively inhibited replication of Chikungunya virus. *Antiviral Res* 134:42–49. DOI:

585   10.1016/j.antiviral.2016.08.019.

586   de los Santos T, Wu Q, de Avila Botton S, Grubman MJ. 2005. Short hairpin RNA targeted to

587   the highly conserved 2B nonstructural protein coding region inhibits replication of

588   multiple serotypes of foot-and-mouth disease virus. *Virology* 335:222–31. DOI:

589   10.1016/j.virol.2005.03.001.

590 Shah PS, Schaffer DV. 2011. Antiviral RNAi: translating science towards therapeutic success.

591   *Pharm Res* 28:2966–82. DOI: 10.1007/s11095-011-0549-8.

592 Tafer H, Ameres SL, Obernosterer G, Gebeshuber CA, Schroeder R, Martinez J, Hofacker IL.

593   2008. The impact of target site accessibility on the design of effective siRNAs. *Nat*

594   *Biotechnol* 26:578–83. DOI: 10.1038/nbt1404.

595 Westerhout EM. 2005. HIV-1 can escape from RNA interference by evolving an alternative

596   structure in its RNA genome. *Nucleic Acids Research* 33:796–804. DOI:

597   10.1093/nar/gki220.

598

599

600

601 **Figure captions**

602

603 Fig. 1 RNAxs results of target prediction within FMDV 3D region. Data are represented as the

604 number of predicted target sequences (coverage) per 3D nucleotide. Total number of predicted

605 sequences (blue areas) and sequences corresponding to the top 50 hits in the RNAxs ranking (red

606 areas) are shown. Target sequences selected for further study are indicated at the top of the

607 corresponding peaks

608

609 Fig. 2 Silencing activity of small RNAs directed against FMDV 3D sequences. Co-transfected

610 cells were trypsinized and EGFP expression was analyzed by flow cytometry at 24 hpi as

611 described in Material and Methods. Cells were co-transfected with pEGFP3D and shRNA$_{FMDV}$

612 (A), amiRNA$_{FMDV}$ (B) or dual amiRNA$_{FMDV}$ (C) expressing plasmids. *p<0.05; **p<0.01;

613 ***p<0.001

614

615 Fig. 3 Antiviral effect of amiRNAs$_{FMDV}$ stably expressed in BHK-21 cells. (A) Cytopathic effect

616 observed in BHK-21 cell lines expressing amiRNA$_{FMDV}$ and control group (cell lines expressing

617 miRneg) at 48 h post-infection. Cellular detachment, rounding, and destruction of the control

618 group were more severe in the control group than in the experimental group (Magnification

619 100×). (B) Morphology and (C) dimensions of lysis plaques produced by FMDV in

620 amiRNA$_{FMDV}$-expressing cell lines and control cells. FMDV infection produced less plaques of

621 smaller dimensions in cell lines expressing amiRNA than in control cells. ***p<0.0001. (D-F)

622 Viral titers in supernatants of infected cells were determined by the $TCID_{50}$ method at 18 hpi

623 (D), 24 hpi (E) or 48 hpi (F). **$p<0.01$.

624

625 Fig. 4 Antiviral activity of cloned $amiRNA_{290}$ (A-C) and $amiRNA_{1055}$ (D-F) cell lines. Cell lines

626 were obtained from polyclonal cell lines by limiting dilution as described in Material and

627 Methods. Cells were infected with FMDV A/Arg/01 at a low moi and viral titers in supernatants

628 at 18 hpi (A, D), 24 hpi (B, E) or 48 hpi (C, F) were determined by end-point dilution. *$p<0.05$

629 (as compared to miRneg cells, Student's *t*-test).

630

631 Supplementary Fig. 1 (A) Local RNA structure in the proximity of selected target sequences.

632 RNA structure was predicted using RNAstructure software and SHAPE data covering a 518-nt

633 region spanning positions 892-1410 of FMDV 3D . Target sequences are indicated in orange.

634 Colored nucleotides in sequences 1055-1075 and 1162-1182 represent SHAPE reactivity (red:

635 0.7-1.0; orange: 0.3-0.7; black: 0.0-0.3; grey: no reactivity data). Nucleotides are numbered

636 according to their position in 3Dpol-coding sequence. (B) Correlation between length and

637 starting position of the accessibility window and shRNA efficacy for the training dataset

638 described in Low et al. (Mol Therapy 20:820-828. 2012, modified with permission). The white

639 box indicates the optimal accessible window reported by the authors, starting at position 14 and

640 with a length of 13 nt. Black boxes represent the target sequences selected in this work (1: 290;

641 2: 444; 3: 1055; 4: 1162). (C) Conservation of selected target sequences among prototypic

642 FMDV strains of endemic pool 7, which includes serotypes A and O (www.foot-and-mouth.org).

643 GenBamk accession numbers of prototypic strains are AY593768.1, AY593780.1, AY593815.1,

644 M10975.1. The target sequence derived from FMDV strain A01L used in this study (GenBank

645 accession No. KY404934) is indicated under each logo.

646 Supplementary Fig. 2 Fluorescence microscopy of BHK-21 cells cotransfected with small RNAs

647 and pEGFP.3D reporter plasmid. (A) $shRNA_{FMDV}$, (B) $amiRNA_{FMDV}$ and dual $amiRNA_{FMDV}$.

648 Magnification 400X

649

650 Supplementary Fig. 3 Sequence similarity of target sequence 1162 between FMDV A/Arg/01

651 and FMDV O/CHA/99 (GenBank Accession Numbers KY404934 and AF506822, respectively).

652

653 Supplementary Fig. 4 Expression of mature amiRNAs in stably transfected cell lines. Total RNA

654 was isolated from BHK-21 cells stably transfected with the corresponding single or dual

655 amiRNA-expressing plasmids, and mature amiRNAs were quantitated by RT-stem loop real time

656 PCR as described by Chen et al (Chen, 2005). Mature $amiRNA_{290}$ (A), $amiRNA_{444}$ (B) and

657 $amiRNA_{1055}$ (C) expression from polycistronic vectors was normalized by glyceraldehyde-3-

658 phosphate deshydrogenase (GAPDH, A, B) or endogenous miRNA-706 (C) and relative

659 expression to the same amiRNA in mono-amiRNA polyclonal cells (horizontal line) was

660 calculated by the $2^{-\Delta\Delta CT}$ method. (D, E) Mature amiRNAs were quantitated in clonal cell lines

661 and relative expression to $amiRNA_{290}$ (D) or $amiRNA_{1055}$ (E) (horizontal lines) was calculated as

662 in (A).

663

664   Supplementary Fig. 5. Partial 3D sequenced from RT-PCR amplified virus present in

665   supernatants of infected clonal amiRNA$_{290}$ (A) and amiRNA$_{1055}$ (B) cell lines at 48 hpi. Target

666   sequences are indicated by a box.

667

Figure 1

RNAxs results of target prediction within FMDV 3D region.

Data are represented as the number of predicted target sequences (coverage) per 3D nucleotide. Total number of predicted sequences (gray areas) and sequences corresponding to the top 50 hits in the RNAxs ranking (dark gray areas) are shown. Target sequences selected for further study are indicated at the top of the corresponding peaks.
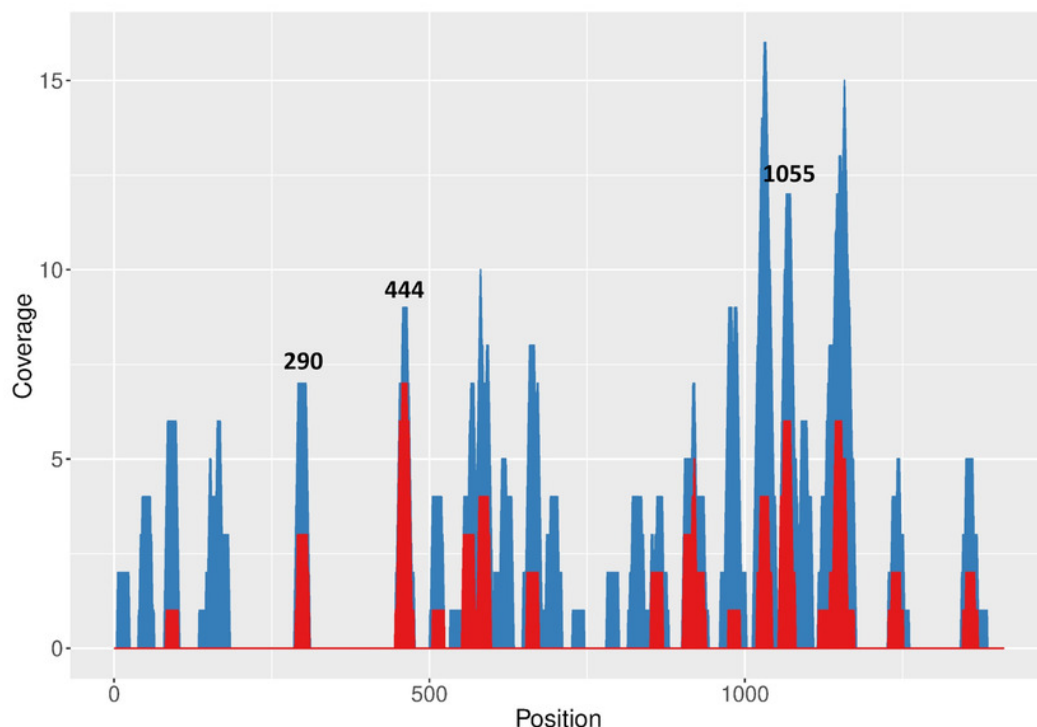
Figure 2

Silencing activity of small RNAs directed against FMDV 3D sequences.

Co-transfected cells were trypsinized and EGFP expression was analyzed by flow cytometry at 24 hpi as described in Material and Methods. Cells were co-transfected with pEGFP3D and shRNA$_{FMDV}$ (A), amiRNA$_{FMDV}$ (B) or dual amiRNA$_{FMDV}$ (C) expressing plasmids. *p<0.05; **p<0.01; ***p<0.001.
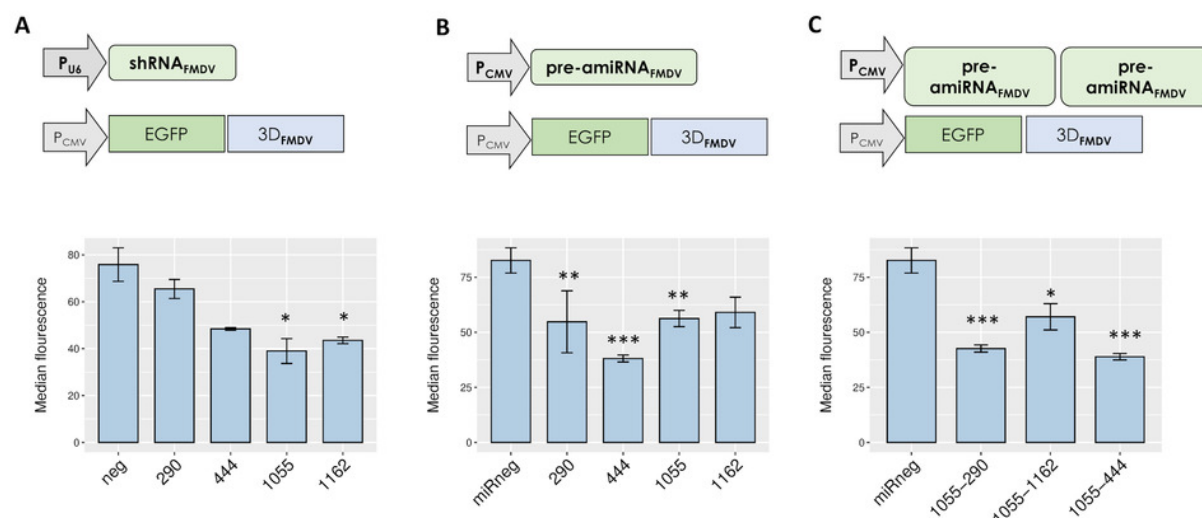
Figure 3

Antiviral effect of amiRNAs$_{FMDV}$ stably expressed in BHK-21 cells.

(A) Cytopathic effect observed in BHK-21 cell lines expressing amiRNA$_{FMDV}$ and control group (cell lines expressing miRneg) at 48 h post-infection. Cellular detachment, rounding, and destruction of the control group were more severe in the control group than in the experimental group (Magnification 100×). (B) Morphology and (C) dimensions of lysis plaques produced by FMDV in amiRNA$_{FMDV}$-expressing cell lines and control cells. FMDV infection produced less plaques of smaller dimensions in cell lines expressing amiRNA than in control cells. ***$p<0.0001$. (D-F) Viral titers in supernatants of infected cells were determined by the TCID$_{50}$ method at 18 hpi (D), 24 hpi (E) or 48 hpi (F). **$p<0.01$.
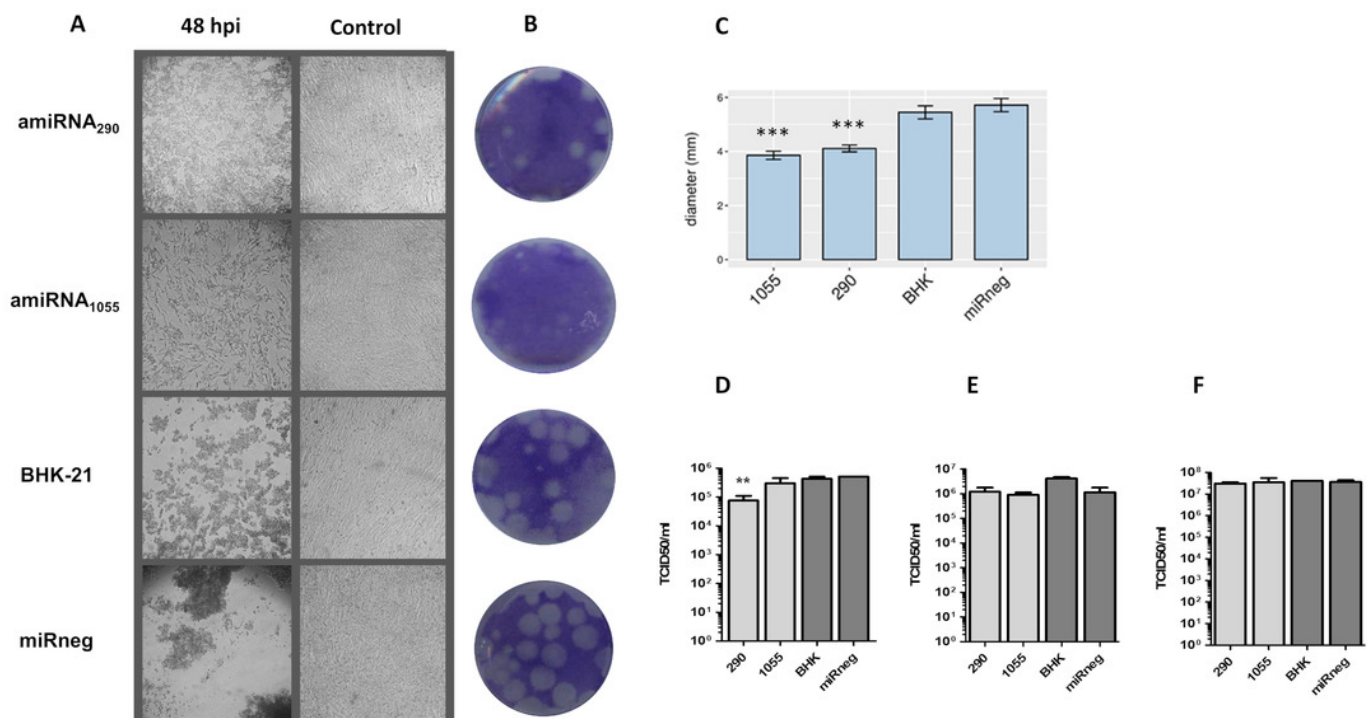
Figure 4

Antiviral activity of cloned amiRNA$_{290}$ (A-C) and amiRNA$_{1055}$ (D-F) cell lines.

Cell lines were obtained from polyclonal cell lines by limiting dilution as described in Material and Methods. Cells were infected with FMDV A/Arg/01 at a low moi and viral titers in supernatants at 18 hpi (A, D), 24 hpi (B, E) or 48 hpi (C, F) were determined by end-point dilution. *p<0.05 (as compared to miRneg cells, Student's *t*-test).
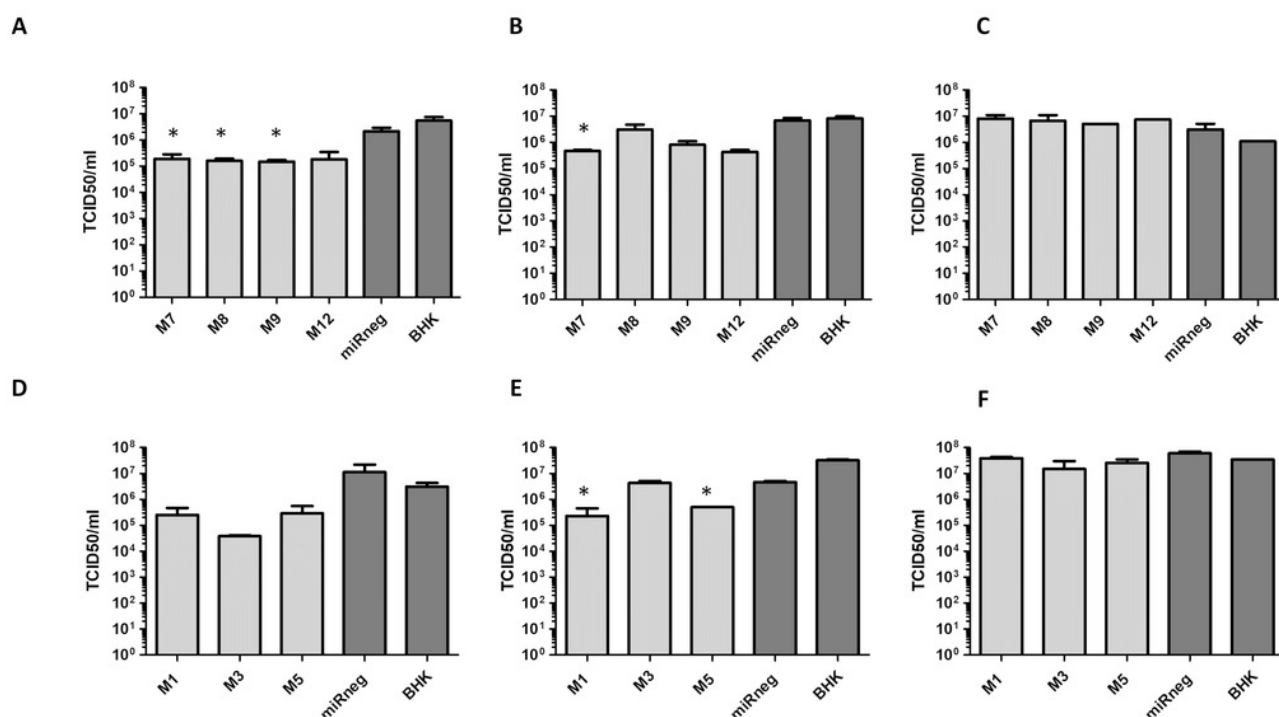
Accessibility parameters of selected target sequences.

Predicted target sequence (5'-3')[a]	Mature sRNA sequence (5'-3')[b]	RNAxs ranking position[c]	Accessible window (starting position; length)	ΔG_{total} (Kcal/mol)[d]	sRNA ID[e]
CGUUUACGAAGCAAUCAAA	**C**UUUGAUUGCUUCGUAAACG**C**	2,3	13; 9	-22.2	290
GGAGAACAGAGAAUACAAA	UAUUCUCUGUUCUCC**AUGAGC***	1,6	17; 5	-22	444
CUCAGGCCCCACUUUAAAU	AUUUAAAGUGGGGCCUGAG**AG**	5	11; 16	-29.6	1055
	AUAGUCCAUGUGGAAGUGUCU		18; 5		1162
	AAAUGUACUGCGCGUGGAGAC				Neg

1 [a] 19 nt target sequences were predicted with RNAxs software.
2 [b] 21 nt target sequences were defined according to the rules described in the Results section. The 2 nucleotides
3 incorporated to the 19 nt predicted sequence are shown in bold.
4 [c] Ranking position of 19 nt predicted target sequences comprised within the 21 nt predicted sRNA sequences.
5 [d] ΔG_{total} was calculated with OligoWalk software, implemented in RNA structure package.
6 [e] sRNAs 1162 and Neg were used as positive and negative controls, respectively.
7 * sRNA$_{444}$ slightly differed from the predicted target sequence to favor a less structured RNA conformation at the
8 target 3' end (Supplementary Figure 1)
9
10

Antiviral activity against FMDV exerted by amiRNAs and shRNAs at 5 hpi.

Target region	% inhibition	
	amiRNA	shRNA
290	96	48
444	90	87
1055	71	77
1162	60	10
1055-290	90	nd
1055-444	74	nd
1055-1162	61	nd

3 nd: not done